Analytical Methods

Accepted Manuscript

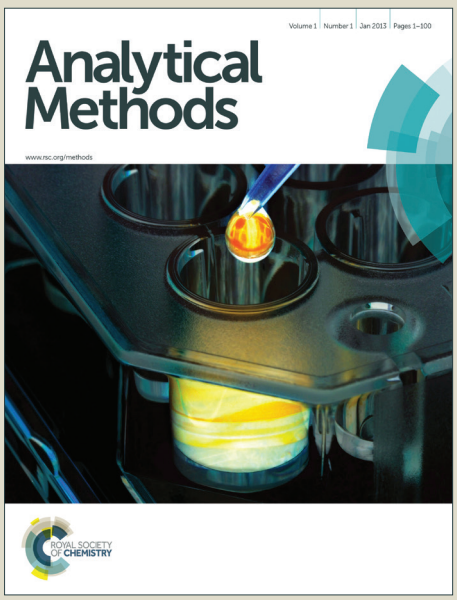

ROYAL SOCIETY OF CHEMISTRY

www.rsc.org/methods

Construction of a nanocomposite sensor by modification of carbon paste electrode with reduced graphene oxide and a hydroquinone derivative: Simultaneous determination of glutathione and penicillamine

Ali Benvidi[a*], Parisa Dehghan[a], Afsaneh Dehghani-Firouzabadi[a], Hamideh Emtiazi[b], Hamid R. Zare[a], Mohammad Mazloum-Ardakani[a]

[a]*Department of Chemistry, Faculty of Science, Yazd University, Yazd 89195-741, Iran*

[b]*Faculty of Parmacy, Shahid Sadoughi University of Medical Science, Yazd, Iran*

Abstract

The present paper reports a sensor for determination of glutathione using a carbon paste electrode modified with reduced graphene oxide (RGO) and 10,10-dimethyl-7(3,4-dihydroxyphenyl)-10,11- dihydrochromeno [4,3-b]chromene-6,8(7H,9H)-dione (DDDC) as a mediator. Graphene nanosheets were obtained by chemical reduction of graphene oxide using hydrazine. Pair of well-defined redox peaks of DDDC was obtained at the modified electrode by direct electron transfer between DDDC and CPE. The novel sensor revealed suitable electrocatalytic activities toward the oxidation of glutathione (Glu). Voltammetric peak currents showed a linear response for Glu in the range of 0.08–100 μM with a detection limit (based on $3s_b/m$) of 0.02 μM. The results exhibited an efficient catalytic activity of the electrode for the electrooxidation of Glu, which led to a reduction in its overpotential by more than 507 mV. In addition, voltammetric investigations of Glu and Penicillamine (PA) showed two separate peaks at the modified electrode, so simultaneous determination of Glu and PA in the real samples was applied at the proposed electrode.

Key words: Reduced graphene oxide, Glutathione, Penicillamine, Carbon paste electrode

1. Introduction

Selectivity, selective preconcentration, electrocatalysis and selective recognition are four important parameters in voltammetric and amperometric modified electrodes [1]. Electrocatalysis at modified electrodes is used for determination of many biological compounds. Some of the important drugs and biosubstrates have an overlapping oxidation potential on unmodified electrodes. Recently, modification of electrodes using nanomaterial and redox

modifiers has significant attention due to reduction of the overpotential essential for electrochemical reaction in electroanalytical chemistry [2-4]. These kinds of electrodes possess many advantages such as low background current, wide range of used potential, easy fabrication, and low expense [5].

Recently, modified electrodes with graphene have attracted main attention because of high electron conductivity and good biocompatibility [6-8]. Graphene sheets, two-dimensional sheets of sp^2 conjugated atomic carbon, have high surface area, excellent electrical conductivity and electron mobility at room temperature. These extra properties of graphene may cause to fabricate novel structures and functionalities.

Glutathione (Glu) is catalyzed by glutathione S-transferase enzyme in cytosol and mitochondria and it is an important antioxidant in plants, animals, fungi, and some bacteria and archaea, preventing damage to important cellular components caused by reactive oxygen species such as free radicals and peroxides [9]. Glu is the major endogenous antioxidant produced by the cells, as well as maintaining exogenous antioxidants such as vitamins C and E in their reduced (active) forms. A number of methods have been reported for the determination of Glu such as spectrophotometry [10], titrimetry [11], spectrofluorimetry [12], capillary zone electrophoresis [13], high performance liquid chromatography (HPLC) [14], flow injection analysis [15], and electrochemical methods [16-19]. Electrochemical methods have shown remarkable advantages in the analysis of different compounds in real samples, due to the simplicity, low cost and relatively short analysis times of compounds as compared to chromatography [20-23]. Glu has been used in selective suppression of skin hyperipigmentation and as antioxidant in the skin lipids protection [24, 25]. Its level in blood serum is directly related with cellular damage, some diseases (e.g., leucocyte loss, psoriasis, liver damage and cancer) and food degradation [26, 27]. So determination of Glu in single human erythrocytes can make benefit clinical diagnosis at the initial stages of disorder.

D-penicillamine (PA), (2*S*)-2-amino-3-methyl-3-sulfanyl-butanoic acid, is the characteristic acid degradation product of β-lactam antibiotics [28] and a chelating agent which is used to aid the elimination of copper in the treatment of hepatolenticular degeneration (Wilson's disease). In Wilson's disease, a rare genetic disorder of copper metabolism, PA treatment relies on its binding to accumulated copper and elimination through urine [29] and has been utilized to treat scleroderma [30]. Also in cystinuria, PA binds with cysteine to yield a mixed disulfide which is

more soluble than cystine [31]. several methodes have been reported for its determination in biological samples due to its biological importance such as fluorimetry [32], chromatography [33], electrophoresis [34] and voltametry [35, 36].

In the present work, we used combination of reduced graphene oxide (RGO) and DDDC in the fabrication of CPE (DDDC/RGO/CPE) for detection of Glu. Modification of electrode with RGO could increase the surface area of electrode and catalytic properties. Due to unique properties of RGO, lower detection limit and wider linear range were obtained compared with other similar sensors. To the best of our knowledge, there have been no report on the fabrication of modified carbon past electrode by synthesized RGO and DDDC for determination of Glu. The experimental results indicate that proposed sensor offers several advantages such as high repeatability, high sensitivity and good stability. The applicability of the modified electrode was successfully demonstrated by voltammetric determination of Glu and simultaneous determination of Glu and PA in real samples such as serum sample and Glu tablet.

2. Experimental

2.1. Apparatus and reagents

The electrochemical experiments were carried out using a potentiostat/galvanostat (SAMA 500, electroanalyzer system I. R. Iran) coupled with a personal computer. A modified electrode (DDDC/RGO/CPE) was used as working electrode. An Ag/AgCl (KCl, sat.) electrode and a platinum wire were used as reference and auxiliary electrodes, respectively. Graphite powder (particle size < 50 μm) from Merck was used as the working electrode (WE) substrate. Glu, PA and other reagents were used with analytical grade (Merck, Darmstadt, Germany). Measurment of pH was carried out using Metrohm model 691 pH/mV meter. Phosphate buffer solutions (0.1 M) were prepared from 0.1 M H_3PO_4–NaH_2PO_4, and pH was regulated with 0.1 M H_3PO_4 or NaOH.

2.2. General procedure for the synthesis of 10,10-dimethyl-7(3,4-dihydroxyphenyl)-10,11-dihydrochromeno[4,3-b]chromene-6,8(7H,9H)-dione

DDDC was synthesized according to the procedure described in the literature [37]. Briefly, a mixture of 4-hydroxycoumarine (1 mmol, 0.162 g), dimedone (1 mmol, 0.140 g), 3,4-dihydroxybenzaldehyde (1 mmol), and $Mg(ClO_4)_2$ (0.04 g) was heated under solvent-free condition in 90°C for appropriate time. After completion of the reaction, for isolation of catalyst

the mixture was dissolved in hot dichloromethane and filtered. The solvent of resulted filtrate was evaporated and the pure product was obtained by recrystalization in ethanol.

Spectroscopic data:

FT- IR: ν_{max} (ATR, neat) = 3400, 2983, 1697, 1665, 1607, 1488, 1364, 1175, 1137, 1058, 897, 767 cm^{-1}. ^{1}H-NMR (500 MHz, DMSO-d_6): δ = 1.01 (s, 3 H), 1.09 (s, 3 H), 2.19 (d, *J*=16.4 Hz, 2H), 2.33 (d, *J*=16.4 Hz, 2H), 2.74 (s, 2H), 4.53 (s, 1H), 6.47 (dd, *J*=8.0 Hz, *J*=2.0 Hz, 1H), 6.57 (d, *J*=8.2 Hz, 1H), 6.68 (d, *J*= 2 Hz, 1H), 7.46 (m, 2H), 7.69 (t, *J*=8.0 Hz, 1H), 7.93 (d, *J*=8.0 Hz, 1H), 8.73 (s, 1H), 8.83 (s, 1H). ^{13}C-NMR (125 MHz, DMSO-d_6) δ = 26.68, 28.50, 31.92, 31.98, 39.58, 50.06, 106.29, 113.17, 114.22, 115.19, 115.89, 116.54, 118.92,122.46, 124.74, 132.63, 133.81, 144.13, 144.69, 151.81, 153.24, 159.94, 162.14, 195.93 ppm.

2.3. Synthesis of reduced graphene oxide

Graphene nanosheets were prepared by oxidizing graphite using an improved method [38]. Briefly, a mixture of concentrated H_2SO_4/H_3PO_4 (360:40 mL) was added to a mixture of graphite/$KMnO_4$ (3:18 g) at 50 °C and stirred for 12 h. The reaction product was cooled to room temperature and transferred into an ice bath and 3 mL 30% H_2O_2 was added to the mixture. The obtained solution was centrifuged and filtered. After that the obtained solution washed with water, 30% HCl, and finally washed twice with 200 mL of ethanol. A suspension of graphene oxide (GO) in purified water (150 mg/50 mL) was prepared by sonication for 3 h. Fig. 1A shows scanning electron microscopy (SEM) of GO. This figure shows that GO has layered structure and homogeneous graphene films. Reduced graphene oxide (RGO) was synthesized using hydrazine and ammonia solution. 50 µL of hydrazine solution (98%) with 200 µL of ammonia solution (30% in water) were added to the suspension of GO, refluxed at 90 °C for 12 h and cooled to room temperature. Subsequently, the solution was centrifuged, and RGO was washed with water and then dried at 60 °C in vacuum for 24 h. Fig. 1B shows SEM image of RGO. This figure shows petal-like graphene nanosheets, extremely sharp edges, and random directions but with a preferred vertical orientation to the substrate, which all resulted in the formation of a nest-like porous structure with a large surface area.

HERE Fig. 1

2.4. Preparation of real sample

Glu tablet solutions were prepared by grinding six glutathione tablets, labeled 100 mg per tablet. Then, 60 mg of tablet powder was weighed and dissolved in 50 mL water by ultrasonication. After that the mixture was filtered on a filter paper. After filtering and adjusting the pH using phosphate buffer (pH 7.0), further dilution was also performed to reach the calibration range of Glu.

The serum sample was centrifuged for 10 min and after filtering with filter paper, was then diluted with PBS with pH 7.0. Ten mL of solution was transferred into the voltammetric cell to be analyzed without any further pretreatment

2.5. Preparation of modified working electrode

To obtain the best conditions in the preparation of DDDC/RGO/CPEs, we optimized the ratio of DDDC, RGO and CPE. The maximum peak current intensity of Glu could be obtained in the optimum condition. In order to prepare DDDC/RGO/CPE a mixture of 0.48 g of graphite powder, 0.005 g of DDDC, 0.015 g of RGO and ~ 0.7 mL of paraffin oil was blended by hand mixing in a mortar and pestle, then the produced paste was inserted in the bottom of a glass tube (internal radius: 2 mm and 10 cm long). When necessary a fresh electrode surface was generated rapidly by extruding a small piece of the paste with a stainless steel rod and smoothing the resulting surface on white paper until a smooth shiny surface was observed.

3. Results and Discussion

3.1. Electrochemical properties of the modified electrode

DDDC/RGO/CPE was prepared and investigated its electrochemical properties in an aqueous solution (pH=7.0) using cyclic voltammetry (CV). Since DDDC is insoluble in aqueous media, therefore it can be incorporated into carbon paste without leaching from the electrode surface. Fig. 2 demonstrates typical CV behaviors of the modified electrode in 0.1 M phosphate buffer (pH=7.0).

Curve A in Fig. 2 shows the effect of the potential scan rate on electrochemical properties of the DDDC/RGO/CPE in 0.1 M phosphate buffer solution. The plots of the anodic and cathodic peak currents (I_p) were linearly dependent on scan rate from 10 mV s^{-1} to 800 mV s^{-1} indicating that the nature of the redox process was controlled in diffusionless manner for a surface-confined redox process [39].

According to the sharp method [40], the peak current is related to the surface concentration of the electroactive species, Γ, by the following equation:

$I_p = n^2F^2A\Gamma v/4RT$ (1)

where n represents the number of electrons involved in the reaction, A is the surface area (0.096 cm^2) of the electrode, Γ (mol cm^{-2}) is the surface coverage, and the other symbols have their usual meanings. From the slope of the anodic peak currents versus the scan rate (Fig. 2A), the calculated surface concentration of DDDC at DDDC/RGO/CPE is 6.26×10^{-8} mol cm^{-2} for $n = 2$.

According to the method of Laviron [41], the apparent charge transfer rate constant, k_s, and the charge transfer coefficient, α, of a surface-confined redox can be evaluated based on the variation of the anodic and cathodic peak potentials of cyclic voltammograms toward the logarithm of the scan rate. Curve B in Fig. 2 shows a variation of E_p versus the logarithm of scan rate. The slopes of the linear segments ($2.303RT/(1- \alpha_a)\ n_\alpha F$ for the anodic peaks and $2.303RT/\alpha_c n_\alpha F$ for the cathodic peaks) in Fig. 2C can be used for extraction of kinetic parameters. The calculated value for the average transfer coefficient (α) is 0.51. The electron transfer rate constant (k_s) between the modifier (DDDC) and CPE can be calculated by using Eq. (2):

$\log k_s = \alpha \log(1 - \alpha) + (1 - \alpha)\log \alpha - \log(RT/n_\alpha Fv) - \alpha(1- \alpha)n_\alpha F\Delta E_p/2.3RT$ (2)

The value of k_s=5.32 s^{-1} was evaluated using eq (2).

HERE Fig. 2

The electrochemical behavior of a DDDC/RGO/GCE at different pH values was studied by CVs. It was observed that the anodic and cathodic peak potentials of DDDC/RGO/GCE shifted to negative values with increasing pH. Inset D of Fig. 2 shows a potential-pH diagram by plotting the calculated half-wave potential values as a function of pH. This diagram is composed of a straight line with a slope of 55.6 mV pH^{-1} in the pH ranges of 3.0–11.0. Therefore, the redox reaction of DDDC behaves the Nernst equation for a two electron and two proton transfer reaction [39].

3.2. Electrocatalytic oxidation of Glu at modified electrode

Fig. 3 shows CV responses of 80.0 μM Glu at CPE (curve a), RGO/CPE (curve b), DDDC/CPE (curve c) and DDDC/RGO/CPE (curve d). Also curves e and f of Fig. 3 shows CV response of DDDC/RGO/CPE and CPE in the buffer solution in absence of Glu, respectively. As it is seen, the anodic peak potential for Glu at bare CPE is 680.0 mV, while the corresponding potential at DDDC/RGO/CPE is about 172 mV (Fig. 3 curve d). The comparison of Glu oxidation at CPE (curve a) and RGO/CPE (curve b) shows an enhancement of the anodic peak current at RGO/CPE (curve b) indicating that the presence of RGO in CPE could enhance the peak current due to excellent characteristics of RGO. Also, in the presence of Glu, the anodic peak current of DDDC is increased and the cathodic peak of the modifier disappears on the reverse scan of the potential. As a results, an EC' catalytic mechanism is suggested for Glu oxidation at the surface of DDDC/RGO/CPE. In this mechanism, Glu is oxidized in the catalytic chemical reaction by DDDC which produced via an electrochemical reaction. Therefore, when DDDC is oxidized at the potential of 172 mV, Glu can be oxidized in this potential, too.

HERE Fig. 3

3.3. The optimization of pH and electrode ingredients

For increasing the sensitivity and selectivity of the proposed electrode for Glu determination, the effect of pH and composition of the electrode materials such as RGO and DDDC were optimized. The effect of pH was investigated on the electrocatalytic oxidation of Glu in a buffered solution containing 80 μM Glu. As inset of Fig. 3 shows the $\Delta I = I_{Glu} - I_0$ (I_{Glu} is anodic peak current in the presence of Glu and I_0 is anodic peak current in the absence of Glu) increased from pH 4.0 to 7.0, and then decreased at higher pH (from 7.0 to 9.0). Therefore, a phosphate buffer solution with pH of 7.0 was selected for further works.

To obtain the maximum peak current for Glu (80.0 μM), the electrode ingredients was optimized. As the Table 1 shows for the first 4 experiments, in the absence of RGO the amount of DDDC modifier was increased. In the three remain experiments the weight percent of RGO was increased while the amount of DDDC was held constant. According to the Table 1 the best ΔI was obtained for compositions of 0.480 g graphite powder, 0.005 g DDDC, 0.015 g RGO and ~ 0.7 mL paraffin oil which corresponds to relative percentage of 1:3:96 for DDDC:RGO:Graphite respectively.

HERE Table 1

3.4. The effect of scan rate and Tafel diagram

Fig. 4 shows CV at 30 mV s^{-1} of DDDC/RGO/CPE in PBS (pH 7.0) containing 80.0 μM Glu. The inset A in Fig. 4 shows a Tafel diagram using the rising part of the cyclic voltammogram. Using the slope of Tafel diagram, a charge transfer coefficient 0.3 for catalytic oxidation of Glu was obtained. The effect of scan rate on the electrocatalytic oxidation of Glu at DDDC/RGO/CPE in PBS (pH 7.0) containing 80.0 μM Glu was investigated by CV (inset B in Fig. 4). As it can be observed, the anodic oxidation current of Glu is proportional to the square root of the scan rate ($v^{1/2}$), suggesting that the reaction is controlled by diffusion of Glu at the surface of electrode [39].

HERE Fig. 4

3. 5. Chronoamperometric studies

Chronoamperometry was employed to investigate the electrochemical behavior of an aqueous buffered solution (pH 7.0) containing various concentrations of Glu at DDDC/RGO/CPE by setting the working electrode potential at 0.280 V. The linearity of the electrocatalytic current vs. $v^{1/2}$ shows that the current is controlled by diffusion of Glu from the bulk solution toward the surface of the electrode that causes a near-Cottrellian behavior. Therefore, the slope of the linear region of the Cottrell's plot can be used to estimate the diffusion coefficient of Glu. A plot of I vs. $t^{-1/2}$ for DDDC/RGO/CPE in the presence of Glu gives a straight line, the slope of which can be used to estimate the diffusion coefficient of Glu (D) (Fig. 5, inset A). The mean value of D was found to be 3.9×10^{-6} cm^2 s^{-1} which is comparable with values reported by other research groups for Glu [41, 42]. Also, we can assay the catalytic rate constant, *k*, from the reduced form of Galus by using equation (Eq. 3) [43].

$$I_{Cat}/I_L = \pi^{1/2}\gamma^{1/2} = \pi^{1/2}(kC_b t)^{1/2} \qquad (3)$$

where I_C is the catalytic current of DDDC/RGO/CPE in the presence of Glu, I_L is the limited current in the absence of Glu, and C_b is the bulk concentration of Glu. Having measured the catalytic current, i.e., I_C, it is possible to carry out the electrode process under identical conditions, but in the absence of Glu, in order to determine I_L. From the slope of I_C/I_L vs. $t^{1/2}$ plot, the value of *k* can be simply calculated for a given concentration of Glu. The calculated value of *k* is $(3.53 \pm 0.08) \times 10^3$ M^{-1} s^{-1} using the slope of I_C/I_L–$t^{1/2}$ plot (Fig. 5, inset B). This

value of *k* also explains the sharp feature of the catalytic peak observed for the catalytic oxidation of Glu at the surface of DDDC/RGO/CPE.

HERE Fig. 5

3. 6. Calibration plot and detection limit using differential pulse voltammetry

Since differential pulse voltammetry (DPV) has a much higher sensitivity and better resolution than cyclic voltammetry, this technique can be examined for determination of linear range and detection limit of Glu by the proposed electrochemical sensor. The effect of pulse height was investigated on the sensitivity of DPV. The results showed that by increasing pulse height, the sensitivity of method increased, but at the pulse heights more than 50 mV, the peak width increased. So, for obtaining more sensitivity and better peak shapes, the pulse height of 50 mV was selected. DPV in optimized condition showed a linear range of 0.08-100.0 μM with a detection limit (based on 3s/m) of 0.02 μM for Glu.

3.7. Simultaneous determination of Glu and PA

To the best of our knowledge, there is no report on the simultaneous determination of Glu and PA using DDDC/RGO/CPE. Therefore, the main objective of this study was to detect Glu and PA simultaneously using DDDC/RGO/CPE. To obtain this aim, DPV technique was applied and the concentrations of Glu and PA were changed simultaneously. The obtained results from DPV show two well-distinguished anodic peaks at potentials of 140 and 430 mV corresponding to the oxidation of Glu and PA, respectively; indicating that simultaneous determination of these compounds is feasible at DDDC/RGO/CPE as shown in Fig. 6. It is interesting to note that the sensitivities of the modified electrode to Glu in the absence and presence of PA are virtually close, which indicates that the oxidation processes of Glu and PA at DDDC/RGO/CPE are independent. The DPV signals showed a linear relationship in the range of 0.5-50.0 μM with a detection limit (based on 3s/m) of 0.06 μM for PA. Therefore, independent or simultaneous measurements of two analyses are possible without any interference.

HERE Fig. 6

3.8. Interference study

In order to evaluate the selectivity of the proposed method for the determination of Glu (10.0 μM), we investigated the influence of various foreign species frequently found with Glu in pharmaceutical. The tolerance limit was taken as the maximum concentration of foreign substances causing an approximately ± 5% relative error in the determination of Glu. The tolerated concentration of foreign substances was 1000.0 μM for Na^{+}, Cl^{-}, Mg^{2+}, K^{+}, Mg^{+2}, and 50.0 μM for glucose, fructose, acetaminophen, folic acid, ascorbic acid and vitamin B6 and uric acid.

3.9. Reproducibility and stability of DDDC/RGO/CPE

The electrode capability for the generation of a reproducible surface was examined by DPV.

Data obtained in optimum solution pH 7.0 from five separately prepared DDDC/RGO/CPE**.** The calculated RSD for DPV peak current in determination of 100 μM Glu solution is about 3.1% for different prepared electrodes indicating that reproducibility of preparation is excellent. The stability of DDDC/RGO/CPE was tested over a five-week period. The modified electrode was rinsed and stored at room temperature after recording DPVs. The peak potential for Glu oxidation was unchanged and the current signals showed a decrease less than 5.2% relative to the initial response after five weeks.

3.10. Determination of Glu and PA in real samples

In order to show the catalytic oxidation of Glu in the real samples, we examined this ability in the voltammetric determination of Glu in a Glu tablet purchased from local sources. The determination of Glu in the tablet samples was carried out by the multi-point standard addition in order to prevent any matrix effect. The amount of unknown Glu in the tablet can be obtained by extrapolating the plot. The average amount of Glu in the tablet was found to be 98 mg with a recovery of 98%, which is in good agreement with the nominal value of the tablet label (100.0 mg). Also, for investigation of the applicability of DDDC/RGO/CPE for simultaneous determination of Glu and PA in real samples, this electrode was applied in serum solutions. Table 2 shows the recovery percent of Glu and PA in serum solutions using DDDC/RGO/CPE which are good for spiked Glu and PA values.

4. Conclusions

This work demonstrates the construction of DDDC/RGO/CPE and its application in Glu determination. The results show that the oxidation of Glu is catalyzed by the mediator at pH 7.0, whereas the peak potential of Glu is shifted by 507 mV to a less positive potential at the surface of DDDC/RGO/CPE. Low detection limit and high precision along with simultaneous determination of Glu and PA are the advantages of the proposed electrode. According to Table 3, obtained results reveal that the detection limit, dynamic linear range, and sensitivity for Glu with the modified electrode is comparable or even better than which obtained by some other applied modified electrodes.

References:

1 Y. Zhang, X. Chen and W. Yang, *Sens. Actuators B: Chem*. 2007, **130,** 682.

2 M. Mazloum Ardakani, N. Rajabzadeh, A. Dehghani Firouzabadi, M. A. Sheikh-Mohseni, A. Benvidi, H. Naeimi, M. Akbari, and A. Karshenas, *Anal methods*, 2012, **4,** 2127.

3 M. Mazloum-Ardakani, N. Rajabzadeh, A. Dehghani Firouzabadi, A. Benvidi and M. Abdollahi-Alibeik, *Anal. Methods*, 2014, **6**, 4462.

4 A. Benvidi, A. Dehghani-Firouzabadi, M. Mazloum-Ardakani and B.B.F. Mirjalili, *J. Electroanal. Chem*. 2014, **736**, 22.

5 M. Mazloum-Ardakani, A. Khoshroo and L. Hosseinzadeh, *Sens. Actuators B*, 2014, **204**, 282.

6 S. Guo, D. Wen, Y. Zhai, S. Dong and E. Wang, *ACS Nano*., 2010, **7**, 3959.

7 Z. Yao, M. Zhu, F. Jiang, Y. Du, C. Wang and P. Yang, *J. Mater. Chem*., 2012, **22**, 13707.

8 F. Cui and X. Zhang, *J. Electroanal. Chem*., 2012, **669**, 35.

9 A. Pompella, A. Visvikis, A. Paolicchi, V. Tata and A. F. *Casini*, 2003, **66**, 1499.

10 K. Kamata, M. Takahashi, K. Terajima and M. Nishijima, *Analyst*, 1995, **120**, 2755.

11 P. Nagendra, H. S. Yathirajan and K. S. Rangappa, *J. Indian Chem. Soc*., 2002, **79,** 602.

12 S. C. Liang, H. Wang, Z. M. Zhang, X. Zhang and H. S. Zhang, *Anal. Chim. Acta*, 2002, **451** 211.

13 E. Causse, P. Malatray, R. Calaf, P. Chariots, M. Candito, C. Bayle, P. Valdiguie, C. Salvayre, F.

14 A.E. Katrusiak, P.G. Paterson and H. Kamencic, *J. Chromatogr. B*., 2001, **758**, 207.

15 A.A. Ensafi, T. Khayamian and F. Hasanpour, *J. Pharma. Biomed. Anal*., 2008, **48**, 140.

16 J.B. Raoof, R. Ojani and H. Karimi-Maleh, *J. Appl. Electrochem*., 2009, **39**, 1169.

17 J.B. Raoof, R. Ojani and M. Kolbadinezhad, *J. Solid State Electrochem*., 2009, **13**, 1411.

18 A.A. Ensafi, M. Taei, T. Khayamian, H. Karimi-Maleh and F. Hasanpour, *J. Solid State Electrochem.,* 2010, **14,** 1415.

19 A.A. Ensafi, S. Dadkhah-Tehrani and H. Karimi-Maleh, *Drug Test. Analysis*., 2011, **3**, 325.

20 H. Beitollahi, M. Mazloum Ardakani, H. Naeimi and B. Ganjipour, *J. Solid State Electrochem,*. 2009, **13**, 353.

21 M. Mazloum-Ardakani, H. Rajabi, B. B. F. Mirjalili, H. Beitollahi and A. Akbari, *J. Solid State Electrochem*., 2010, **14,** 2285.

22 M. Mazloum Ardakani, H. Beitollahi, Z. Taleat and M. Salavati-Niasari, *J. Serb. Chem. Soc*., 2011, **76**, 575.

23 H. Karimi-Maleh, M. Keyvanfard, K. Alizad, V. Khosravi, M. Asnaashariisfahani, *Int. J. Electrochem. Sci.,* 2012, **7**, 6816.

24 R. Moradi, S. A, Sebt, H. Karimi-Maleh, R. Sadeghi, F. Karimi, A. Bahari and H. Arabi *Phys Chem Chem Phys*, 2013, **15**, 5888.

25 G. Devi, M. Prasad , I. Saraswathi, D. Raghu, D. Rao, P.P. Reddy, *Clin Chim Acta*, 2000, **93**, 53.

26 I. Rahman, A. Kode and S. K. Biswas, *Nat. Protoc*., 2007, **1**, 3159.

27 Y. Wang, J. Lu, L. H. Tang, H. X. Chang and J. H. Li, *Anal. Chem*., 2009, **81**, 9710.

28 A. Ghaffarinejad, F. Hashemi, Z. Nodehi and R. Salahandish, *Bioelectrochem.,* 2014, **99**, 53.

29 J. Peisach, W. E. Blumberg, *Molecular pharmacology.*, 1969, **5**, 200.

30 L. E. Rosenberg, and J. P. Hayslett, *JAM.,* 1967*,* **201**, 698

31 V. D. Steen, J. Medsger, and , G. P. Rodnan, *Annals of internal medicine,* 1982 **97**, 652.

32 R. A. Shaalan, *Cent. Eur. J. Chem*., 2010, **8,** 892.

33 M.A. Saracino, C. Cannistraci, F. Bugamelli, E. Morganti, I. Neri, R. Balestri, A. Patrizi, and M.A. Raggi, *Talanta.*, 2013, **103**, 355.

34 L. Song, Z. Guo and Y. Chen, *Electrophoresis.,* 2012, **3**, 2056.

35 M. Mazloum-Ardakani, M. A. Sheikh-Mohseni and B. F. Mirjalili, *Electroanalysis,* 2013, **25** 2021.

36 M. Amiri, K. Nekoiean and A. Bezaatpour, *Electroanalysis.,* 2012, **24**, 2186.

37 H. Emtiazi, M. A. Amrollahi, *S. Afr. J. Chem*, 2014, **67**, 175.

38 D. C. Marcano, D. V. Kosynkin, J. M. Berlin, A. Sinitskii, Z. Sun, A. Slesarev, L. B. Alemany, W. Lu and M. Tour, *ACS Nano*, 2010, **4**, 4806.

39 A. J. Bard and L. R. Faulkner, Electrochemical methods: fundamentals and applications, 2nd ed. Wiley, New York. 2001.

40 M. Sharp, M. Petersson and K. Edstrom. *J. Electroanal. chem*, 1979, **95**,123.

41 M. Keyvanfard, H. Karimi-Maleh and K. Aliza, *Chin. J. Catal.,* 2013, **34,** 1883.

42 J. J. Ruiz-Diaz, A. A. Torriero, E. Salinas, E. J. Marchevsky, M. I. Sanz and J. Raba, *Talanta*, 2006, **68**, 1343.

43 Z. Galus, Fundamentals of Electrochemical Analysis, Ellis Horwood, New York, 1976.

44 H. Karimi-Maleh, M. Keyvanfard, K. Aliza, V. Khosravi and Ma. Asnaashari isfahani, *Int. J. Electrochem. Sci*., 2012, **7**, 6816.

Caption of figures:

Fig. 1 SEM images of A) GO and B) RGO

Fig. 2 Cyclic voltammograms obtained at DDDC/RGO/CPE in a 0.1 M phosphate buffer solution (pH 7.0) at various scan rates from 10 to 800 mV s^{-1}. Insets: (A) Variations of I_{pa} versus scan rate (B) Variation of E versus the logarithm of scan rate, (C) Variation of E versus the logarithm of scan rate for high scan rate

Fig. 3 Cyclic voltammograms obtained at (a) CPE (b) RGO/CPE (c) DDDC/CPE and (d) DDDC/RGO/CPE in a 0.1 M phosphate buffer solution (pH 7.0) containing 80.0 μM Glu at a scan rate of 30 mVs^{-1}, CVs obtained at (e) DDDC/RGO/CPE and (f) CPE in a 0.1 M phosphate buffer solution (pH 7.0), Inset: Effect of pH on the oxidation peak current of Glu.

Fig. 4 CV obtained at DDDC/RGO/CPE in a 0.1 M phosphate buffer solution (pH 7.0), containing 80.0 μM Glu at a scan rate of 30 mV s^{-1}, inset (A) The Tafel plot derived from the CV at scan rate 30 mV s^{-1} and inset (B) Variation of the electrocatalytic currents vs. the square root of the scan rate

Fig. 5 Chronoamperograms obtained at DDDC/RGO/CPE in a 0.1 M phosphate buffer solution (pH 7.0) for Glu concentrations of 0.0, 0.1, 0.2, 0.4, 0.6 and 0.8 mM. Insets: (A) plots of I vs. $t^{-1/2}$ obtained from the chronoamperogram data, (B) plot of the slope of the straight lines against the Glu concentration and (C) dependence of I_C/I_L derived from the data of chronoamperograms vs. $t^{-1/2}$

Fig. 6 DPV obtained for DDDC/RGO/CPE in a 0.1 M phosphate buffer solution (pH 7.0) containing different concentrations of Glu and PA (from inner to outer) mixed solutions of 20.0+0.5, 40.0+2.0, 60.0+5.0, 80.0+10.0 and 100.0+20.0 μM, respectively. Insets: A) plot of the peak current as a function of Glu concentration and B) Plot of the peak current as a function of PA concentration

Table 1: The effect of the electrode ingredients on the Glu oxdidation peak current

Graphite%	RGO%	DDDC%	ΔI (μA)
99.75	0	0.25	3.2
99.5	0	0.5	4.2
99.0	0	1	4.4
98.5	0	1.5	4.3
98.0	1	1	5.2
97.0	2	1	6.4
96.0	3	1	6.5

Table 2 Determination of Glu and PA in the serum sample using DDDC/RGO/CPE

Sample	spiked (μM)		Found (μM) [a]		Recovery (%)	
	Glu	PA	Glu	PA	Glu	PA
1	0.0	0.0	1.2	ND[b]	-	-
2	10.0	5.0	10.7	5.2	95.0±3.1	104.0±1.2
3	20.0	10.0	21.5	9.5	101.4±1.2	95.0±2.2
4	50.0	20.0	49.0	19.8	95.7±3.1	99.0±1.8

[a] mean value for five replicate measurements

[b] Not detect

Table 3 Comparison of some used electrochemical procedures for determination of Glu

Electrode	Modifier	pH	Linear range (μM)	Detection limit (μM)	Sensitivity (μA μM^{-1})	Ref
Glassy Carbon	Chlorpromazine	4.0	0.3-18.3	0.16	0.541	[18]
MWCNAT/CPE	3, 4-Dihydroxy-cinamic acid	5.0	0.5-400.0	0.1	3.4346	[41]
Glassy Carbon	Horseradish peroxidase	7.0	0.04-90.0	0.03	0.024	[42]
MWCNAT/ CPE	Isoprenalin	4.0	0.5-300.0	0.09	0.099	[44]
CPE	DDDC[1]/ RGO	7.0	0.08-100.0	0.02	0.043	This work

[1]10,10-dimethyl-7(3,4-dihydroxyphenyl)-10,11- dihydrochromeno[4,3-b]chromene-6,8(7H,9H)-dione

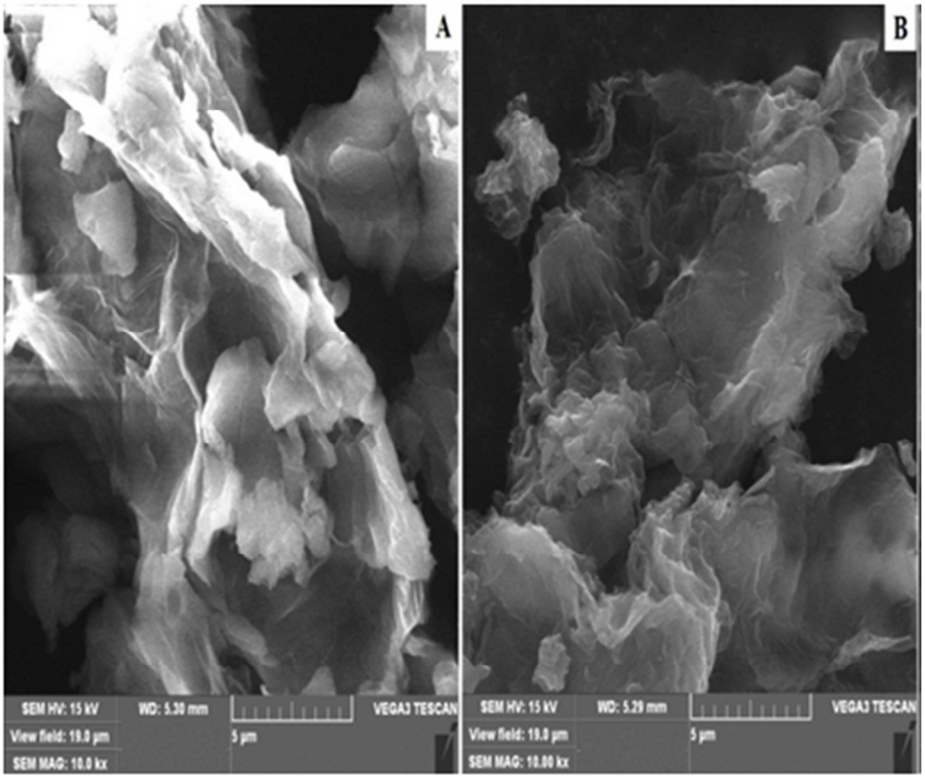

Fig. 1

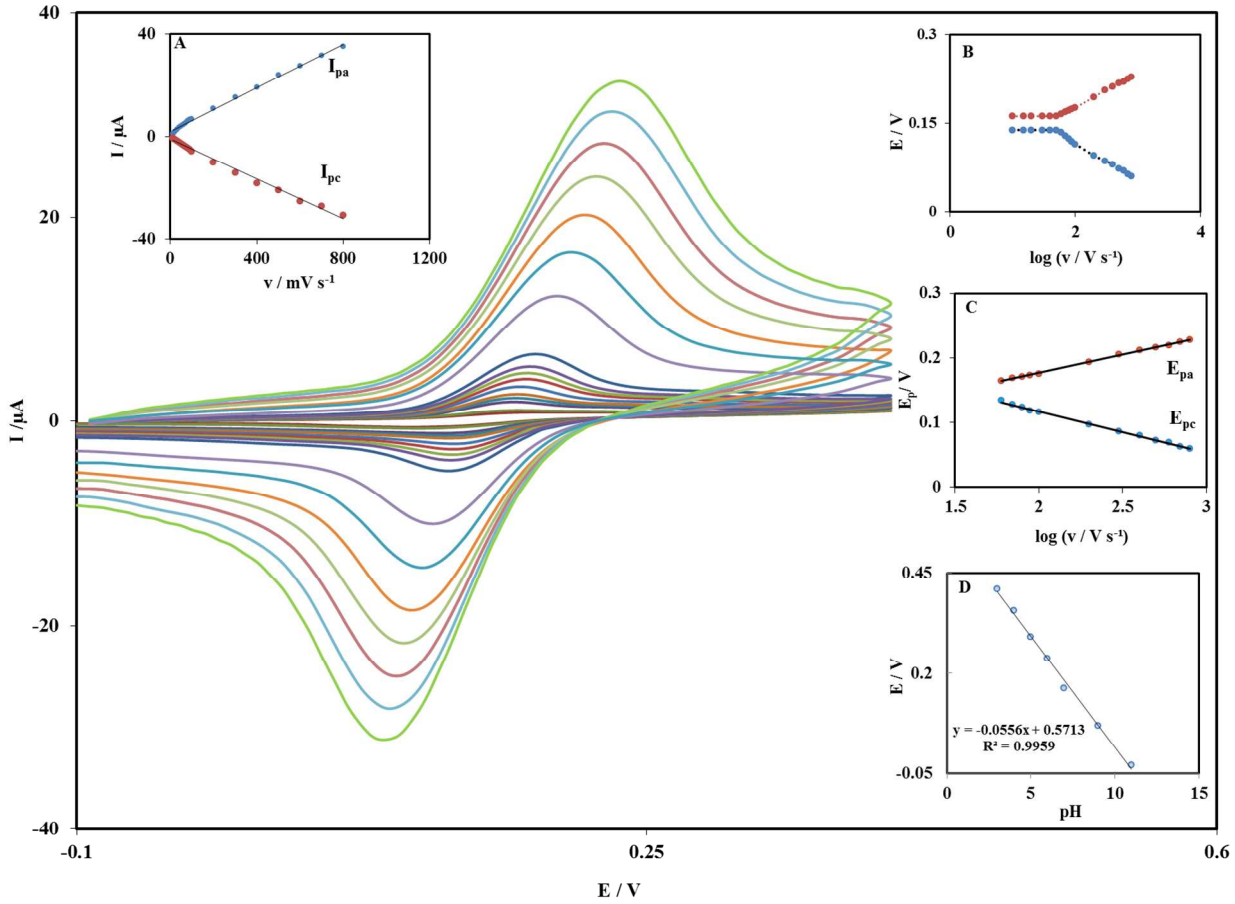

Fig. 2

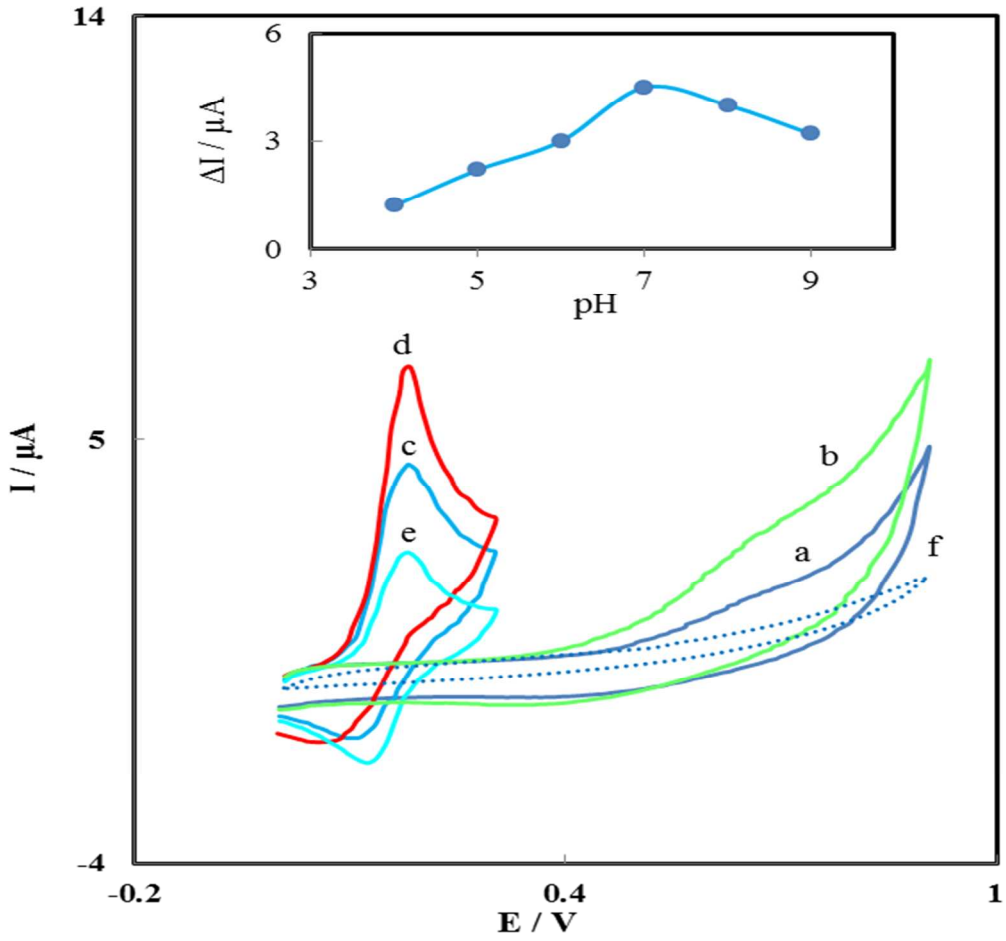

Fig. 3

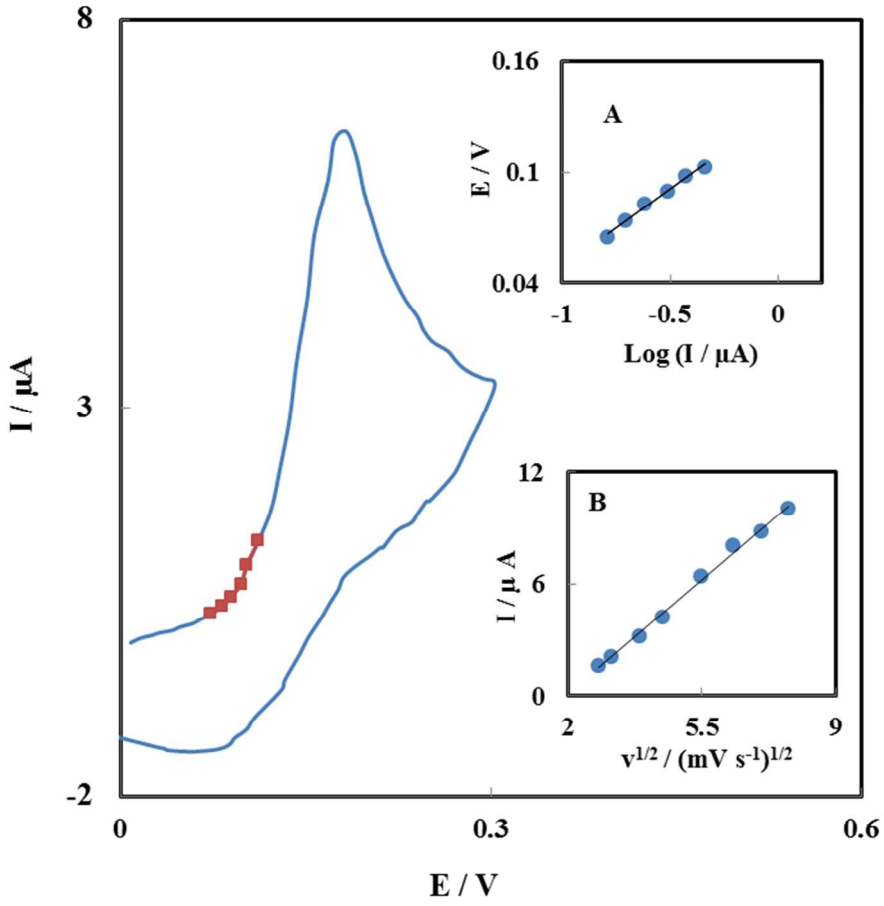

Fig. 4

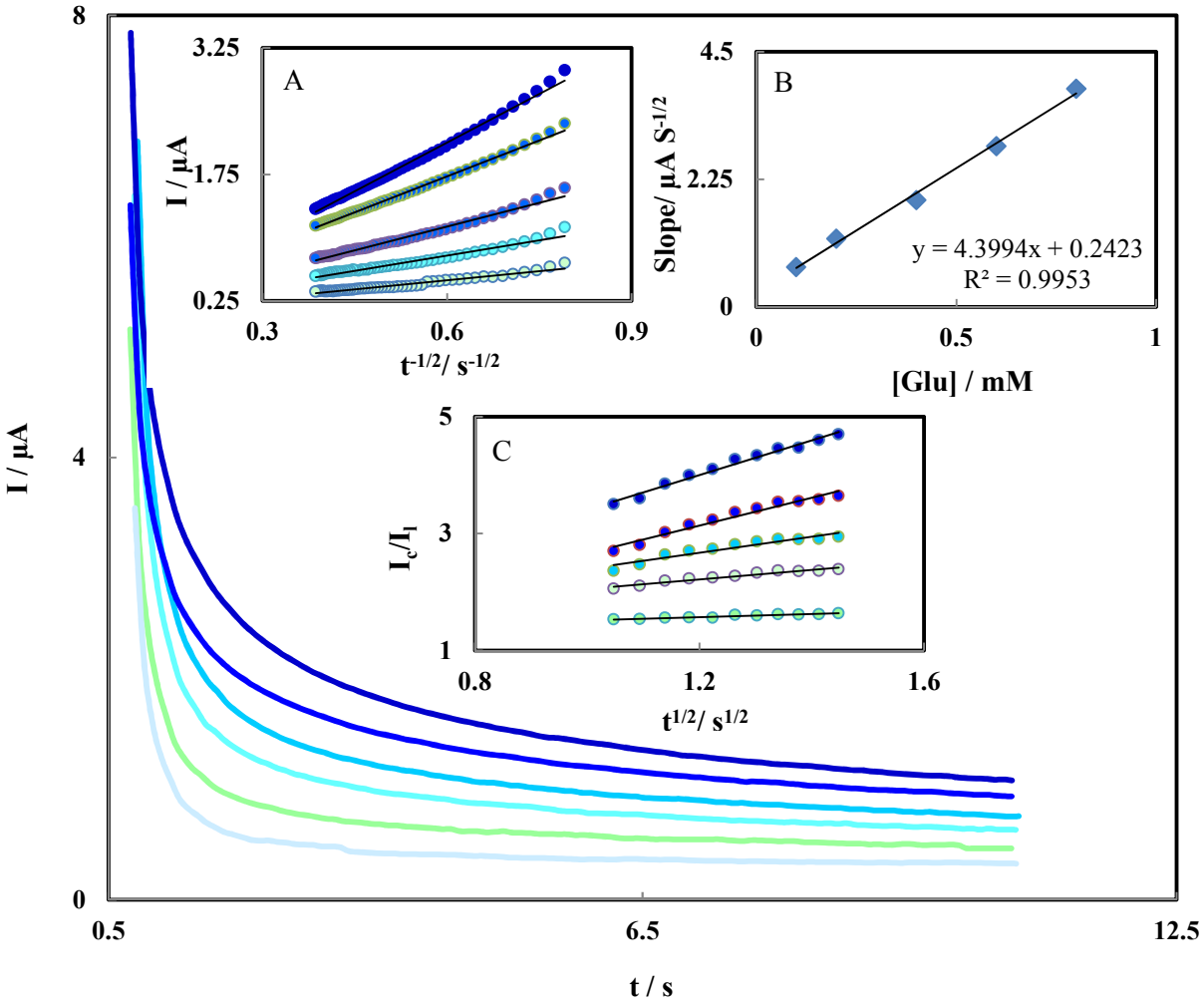

Fig. 5

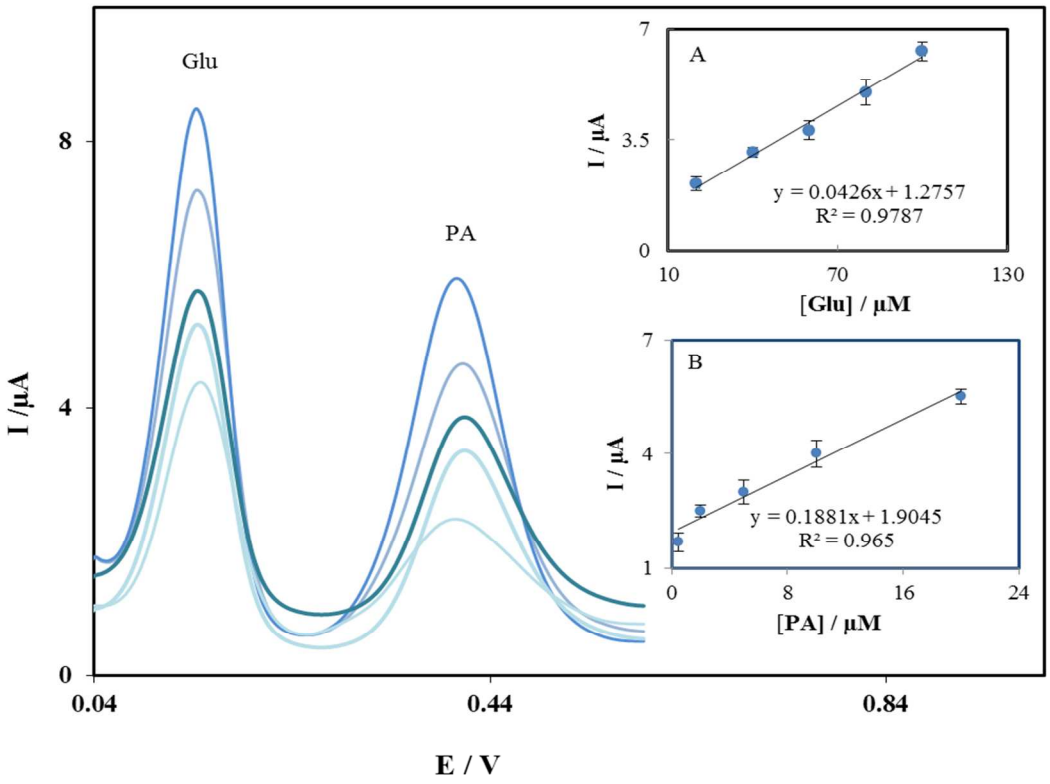

Fig. 6